Measurement of the Top-Quark Mass with Dilepton Events Selected Using Neuroevolution at CDF

T. Aaltonen,[23] J. Adelman,[13] T. Akimoto,[56] M. G. Albrow,[17] B. Álvarez González,[11] S. Amerio,[44b,44a] D. Amidei,[34] A. Anastassov,[38] A. Annovi,[19] J. Antos,[14] G. Apollinari,[17] A. Apresyan,[49] T. Arisawa,[58] A. Artikov,[15] W. Ashmanskas,[17] A. Attal,[4] A. Aurisano,[54] F. Azfar,[42] P. Azzurri,[47d,47a] W. Badgett,[17] A. Barbaro-Galtieri,[28] V. E. Barnes,[49] B. A. Barnett,[25] V. Bartsch,[30] G. Bauer,[32] P.-H. Beauchemin,[33] F. Bedeschi,[47a] P. Bednar,[14] D. Beecher,[30] S. Behari,[25] G. Bellettini,[47b,47a] J. Bellinger,[60] D. Benjamin,[16] A. Beretvas,[17] J. Beringer,[28] A. Bhatti,[51] M. Binkley,[17] D. Bisello,[44b,44a] I. Bizjak,[30] R. E. Blair,[2] C. Blocker,[6] B. Blumenfeld,[25] A. Bocci,[16] A. Bodek,[50] V. Boisvert,[50] G. Bolla,[49] D. Bortoletto,[49] J. Boudreau,[48] A. Boveia,[10] B. Brau,[10] A. Bridgeman,[24] L. Brigliadori,[44a] C. Bromberg,[35] E. Brubaker,[13] J. Budagov,[15] H. S. Budd,[50] S. Budd,[24] K. Burkett,[17] G. Busetto,[44b,44a] P. Bussey,[21,r] A. Buzatu,[33] K. L. Byrum,[2] S. Cabrera,[16,q] C. Calancha,[31] M. Campanelli,[35] M. Campbell,[34] F. Canelli,[17] A. Canepa,[44] D. Carlsmith,[60] R. Carosi,[47a] S. Carrillo,[18,k] S. Carron,[33] B. Casal,[11] M. Casarsa,[17] A. Castro,[6b,6a] P. Catastini,[47c,47a] D. Cauz,[55b,55a] V. Cavaliere,[47c,47a] M. Cavalli-Sforza,[4] A. Cerri,[28] L. Cerrito,[30,o] S. H. Chang,[27] Y. C. Chen,[1] M. Chertok,[7] G. Chiarelli,[47a] G. Chlachidze,[17] F. Chlebana,[17] K. Cho,[27] D. Chokheli,[15] J. P. Chou,[22] G. Choudalakis,[32] S. H. Chuang,[53] K. Chung,[12] W. H. Chung,[60] Y. S. Chung,[50] C. I. Ciobanu,[43] M. A. Ciocci,[47c,47a] A. Clark,[20] D. Clark,[6] G. Compostella,[44a] M. E. Convery,[17] J. Conway,[7] K. Copic,[34] M. Cordelli,[19] G. Cortiana,[44b,44a] D. J. Cox,[7] F. Crescioli,[47b,47a] C. Cuenca Almenar,[7,q] J. Cuevas,[11,n] R. Culbertson,[17] J. C. Cully,[34] D. Dagenhart,[17] M. Datta,[17] T. Davies,[21] P. de Barbaro,[50] S. De Cecco,[52a] A. Deisher,[28] G. De Lorenzo,[4] M. Dell'Orso,[47b,47a] C. Deluca,[4] L. Demortier,[51] J. Deng,[16] M. Deninno,[6a] P. F. Derwent,[17] G. P. di Giovanni,[43] C. Dionisi,[52b,52a] B. Di Ruzza,[55b,55a] J. R. Dittmann,[5] M. D'Onofrio,[4] S. Donati,[47b,47a] P. Dong,[8] J. Donini,[44a] T. Dorigo,[44a] S. Dube,[53] J. Efron,[39] A. Elagin,[54] R. Erbacher,[7] D. Errede,[24] S. Errede,[24] R. Eusebi,[17] H. C. Fang,[28] S. Farrington,[42] W. T. Fedorko,[13] R. G. Feild,[61] M. Feindt,[26] J. P. Fernandez,[31] C. Ferrazza,[47d,47a] R. Field,[18] G. Flanagan,[49] R. Forrest,[7] M. Franklin,[22] J. C. Freeman,[17] I. Furic,[18] M. Gallinaro,[52a] J. Galyardt,[12] F. Garberson,[10] J. E. Garcia,[47a] A. F. Garfinkel,[49] K. Genser,[17] H. Gerberich,[24] D. Gerdes,[34] A. Gessler,[26] S. Giagu,[52b,52a] V. Giakoumopoulou,[3] P. Giannetti,[47a] K. Gibson,[48] J. L. Gimmell,[50] C. M. Ginsburg,[17] N. Giokaris,[3] M. Giordani,[55b,55a] P. Giromini,[19] M. Giunta,[47b,47a] G. Giurgiu,[25] V. Glagolev,[15] D. Glenzinski,[17] M. Gold,[37] N. Goldschmidt,[18] A. Golossanov,[17] G. Gomez,[11] G. Gomez-Ceballos,[32] M. Goncharov,[54] O. González,[31] I. Gorelov,[37] A. T. Goshaw,[16] K. Goulianos,[51] A. Gresele,[44b,44a] S. Grinstein,[22] C. Grosso-Pilcher,[13] R. C. Group,[17] U. Grundler,[24] J. Guimaraes da Costa,[22] Z. Gunay-Unalan,[35] C. Haber,[28] K. Hahn,[32] S. R. Hahn,[17] E. Halkiadakis,[53] B.-Y. Han,[50] J. Y. Han,[50] R. Handler,[60] F. Happacher,[19] K. Hara,[56] D. Hare,[53] M. Hare,[57] S. Harper,[42] R. F. Harr,[59] R. M. Harris,[17] M. Hartz,[48] K. Hatakeyama,[51] J. Hauser,[8] C. Hays,[42] M. Heck,[26] A. Heijboer,[44] B. Heinemann,[28] J. Heinrich,[44] C. Henderson,[32] M. Herndon,[60] J. Heuser,[26] S. Hewamanage,[5] D. Hidas,[16] C. S. Hill,[10,d] D. Hirschbuehl,[26] A. Hocker,[17] S. Hou,[1] M. Houlden,[29] S.-C. Hsu,[9] B. T. Huffman,[42] R. E. Hughes,[39] U. Husemann,[61] J. Huston,[35] J. Incandela,[10] G. Introzzi,[47a] M. Iori,[52b,52a] A. Ivanov,[7] E. James,[17] B. Jayatilaka,[16] E. J. Jeon,[27] M. K. Jha,[6a] S. Jindariani,[17] W. Johnson,[7] M. Jones,[49] K. K. Joo,[27] S. Y. Jun,[12] J. E. Jung,[27] T. R. Junk,[17] T. Kamon,[54] D. Kar,[18] P. E. Karchin,[59] Y. Kato,[41] R. Kephart,[17] J. Keung,[44] V. Khotilovich,[54] B. Kilminster,[39] D. H. Kim,[27] H. S. Kim,[27] J. E. Kim,[27] M. J. Kim,[19] S. B. Kim,[27] S. H. Kim,[56] Y. K. Kim,[13] N. Kimura,[56] L. Kirsch,[6] S. Klimenko,[18] B. Knuteson,[32] B. R. Ko,[16] S. A. Koay,[10] K. Kondo,[58] D. J. Kong,[27] J. Konigsberg,[18] A. Korytov,[18] A. V. Kotwal,[16] M. Kreps,[26] J. Kroll,[44] D. Krop,[13] N. Krumnack,[5] M. Kruse,[16] V. Krutelyov,[10] T. Kubo,[56] T. Kuhr,[26] N. P. Kulkarni,[59] M. Kurata,[56] Y. Kusakabe,[58] S. Kwang,[13] A. T. Laasanen,[49] S. Lami,[47a] S. Lammel,[17] M. Lancaster,[30] R. L. Lander,[7] K. Lannon,[39] A. Lath,[53] G. Latino,[47c,47a] I. Lazzizzera,[44b,44a] T. LeCompte,[2] E. Lee,[54] S. W. Lee,[54,p] S. Leone,[47a] J. D. Lewis,[17] C. S. Lin,[28] J. Linacre,[42] M. Lindgren,[17] E. Lipeles,[9] A. Lister,[7] D. O. Litvintsev,[17] C. Liu,[48] T. Liu,[17] N. S. Lockyer,[44] A. Loginov,[61] M. Loreti,[44b,44a] L. Lovas,[14] R.-S. Lu,[1] D. Lucchesi,[44b,44a] J. Lueck,[26] C. Luci,[52b,52a] P. Lujan,[28] P. Lukens,[17] G. Lungu,[51] L. Lyons,[42] J. Lys,[28] R. Lysak,[14] E. Lytken,[49] P. Mack,[26] D. MacQueen,[33] R. Madrak,[17] K. Maeshima,[17] K. Makhoul,[32] T. Maki,[23] P. Maksimovic,[25] S. Malde,[42] S. Malik,[30] G. Manca,[29,s] A. Manousakis-Katsikakis,[3] F. Margaroli,[49] C. Marino,[26] C. P. Marino,[24] A. Martin,[61] V. Martin,[21,j] M. Martínez,[4] R. Martínez-Ballarín,[31] T. Maruyama,[56] P. Mastrandrea,[52a] T. Masubuchi,[56] M. E. Mattson,[59] P. Mazzanti,[6a] K. S. McFarland,[50] P. McIntyre,[54] R. McNulty,[29,i] A. Mehta,[29] P. Mehtala,[23] A. Menzione,[47a] P. Merkel,[49] C. Mesropian,[51] T. Miao,[17] N. Miladinovic,[6] R. Miller,[35] C. Mills,[22] M. Milnik,[26] A. Mitra,[1] G. Mitselmakher,[18] H. Miyake,[56] N. Moggi,[6a] C. S. Moon,[27] R. Moore,[17] M. J. Morello,[47b,47a] J. Morlok,[26] P. Movilla Fernandez,[17] J. Mülmenstädt,[28] A. Mukherjee,[17] Th. Muller,[26] R. Mumford,[25]

P. Murat,[17] M. Mussini,[6b,6a] J. Nachtman,[17] Y. Nagai,[56] A. Nagano,[56] J. Naganoma,[58] K. Nakamura,[56] I. Nakano,[40]
A. Napier,[57] V. Necula,[16] C. Neu,[44] M. S. Neubauer,[24] J. Nielsen,[28,f] L. Nodulman,[2] M. Norman,[9] O. Norniella,[24]
E. Nurse,[30] L. Oakes,[42] S. H. Oh,[16] Y. D. Oh,[27] I. Oksuzian,[18] T. Okusawa,[41] R. Orava,[23] K. Osterberg,[23]
S. Pagan Griso,[44b,44a] C. Pagliarone,[47a] E. Palencia,[17] V. Papadimitriou,[17] A. Papaikonomou,[26] A. A. Paramonov,[13]
B. Parks,[39] S. Pashapour,[33] J. Patrick,[17] G. Pauletta,[55b,55a] M. Paulini,[12] C. Paus,[32] D. E. Pellett,[7] A. Penzo,[55a]
T. J. Phillips,[16] G. Piacentino,[47a] E. Pianori,[44] L. Pinera,[18] K. Pitts,[24] C. Plager,[8] L. Pondrom,[60] O. Poukhov,[15,a]
N. Pounder,[42] F. Prakoshyn,[15] A. Pronko,[17] J. Proudfoot,[2] F. Ptohos,[17,h] E. Pueschel,[12] G. Punzi,[47b,47a] J. Pursley,[60]
J. Rademacker,[42,d] A. Rahaman,[48] V. Ramakrishnan,[60] N. Ranjan,[49] I. Redondo,[31] B. Reisert,[17] V. Rekovic,[37] P. Renton,[42]
M. Rescigno,[52a] S. Richter,[26] F. Rimondi,[6b,6a] L. Ristori,[47a] A. Robson,[21] T. Rodrigo,[11] T. Rodriguez,[44] E. Rogers,[24]
S. Rolli,[57] R. Roser,[17] M. Rossi,[55a] R. Rossin,[10] P. Roy,[33] A. Ruiz,[11] J. Russ,[12] V. Rusu,[17] H. Saarikko,[23] A. Safonov,[54]
W. K. Sakumoto,[50] O. Saltó,[4] L. Santi,[55b,55a] S. Sarkar,[52b,52a] L. Sartori,[47a] K. Sato,[17] A. Savoy-Navarro,[43] T. Scheidle,[26]
P. Schlabach,[17] A. Schmidt,[26] E. E. Schmidt,[17] M. A. Schmidt,[13] M. P. Schmidt,[61,a] M. Schmitt,[38] T. Schwarz,[7]
L. Scodellaro,[11] A. L. Scott,[10] A. Scribano,[47c,47a] F. Scuri,[47a] A. Sedov,[49] S. Seidel,[37] Y. Seiya,[41] A. Semenov,[15]
L. Sexton-Kennedy,[17] A. Sfyrla,[20] S. Z. Shalhout,[59] T. Shears,[29] R. Shekhar,[16] P. F. Shepard,[48] D. Sherman,[22]
M. Shimojima,[56,m] S. Shiraishi,[13] M. Shochet,[13] Y. Shon,[60] I. Shreyber,[36] A. Sidoti,[47a] P. Sinervo,[33] A. Sisakyan,[15]
A. J. Slaughter,[17] J. Slaunwhite,[39] K. Sliwa,[57] J. R. Smith,[7] F. D. Snider,[17] R. Snihur,[33] A. Soha,[7] S. Somalwar,[53] V. Sorin,[35]
J. Spalding,[17] T. Spreitzer,[33] P. Squillacioti,[47c,47a] M. Stanitzki,[61] R. St.Denis,[21] B. Stelzer,[8] O. Stelzer-Chilton,[42]
D. Stentz,[38] J. Strologas,[37] D. Stuart,[10] J. S. Suh,[27] A. Sukhanov,[18] I. Suslov,[15] T. Suzuki,[56] A. Taffard,[24,e] R. Takashima,[40]
Y. Takeuchi,[56] R. Tanaka,[40] M. Tecchio,[34] P. K. Teng,[1] K. Terashi,[51] J. Thom,[17,g] A. S. Thompson,[21] G. A. Thompson,[24]
E. Thomson,[44] P. Tipton,[61] V. Tiwari,[12] S. Tkaczyk,[17] D. Toback,[54] S. Tokar,[14] K. Tollefson,[35] T. Tomura,[56] D. Tonelli,[17]
S. Torre,[19] D. Torretta,[17] P. Totaro,[55b,55a] S. Tourneur,[43] Y. Tu,[44] N. Turini,[47c,47a] F. Ukegawa,[56] S. Vallecorsa,[20]
N. van Remortel,[23,b] A. Varganov,[34] E. Vataga,[47d,47a] F. Vázquez,[18,k] G. Velev,[17] C. Vellidis,[3] V. Veszpremi,[49] M. Vidal,[31]
R. Vidal,[17] I. Vila,[11] R. Vilar,[11] T. Vine,[30] M. Vogel,[37] I. Volobouev,[28,p] G. Volpi,[47b,47a] F. Würthwein,[9] P. Wagner,[2]
R. G. Wagner,[2] R. L. Wagner,[17] J. Wagner-Kuhr,[26] W. Wagner,[26] T. Wakisaka,[41] R. Wallny,[8] S. M. Wang,[1] A. Warburton,[33]
D. Waters,[30] M. Weinberger,[54] W. C. Wester III,[17] B. Whitehouse,[57] D. Whiteson,[44,e] S. Whiteson,[16,t] A. B. Wicklund,[2]
E. Wicklund,[17] G. Williams,[33] H. H. Williams,[44] P. Wilson,[17] B. L. Winer,[39] P. Wittich,[17,g] S. Wolbers,[17] C. Wolfe,[13]
T. Wright,[34] X. Wu,[20] S. M. Wynne,[29] S. Xie,[32] A. Yagil,[9] K. Yamamoto,[41] J. Yamaoka,[53] U. K. Yang,[13,l] Y. C. Yang,[27]
W. M. Yao,[28] G. P. Yeh,[17] J. Yoh,[17] K. Yorita,[13] T. Yoshida,[41] G. B. Yu,[50] I. Yu,[27] S. S. Yu,[17] J. C. Yun,[17] L. Zanello,[52b,52a]
A. Zanetti,[55a] I. Zaw,[22] X. Zhang,[24] Y. Zheng,[8,c] and S. Zucchelli[6b,6a]

(CDF Collaboration)

[1]*Institute of Physics, Academia Sinica, Taipei, Taiwan 11529, Republic of China*
[2]*Argonne National Laboratory, Argonne, Illinois 60439, USA*
[3]*University of Athens, 157 71 Athens, Greece*
[4]*Institut de Fisica d'Altes Energies, Universitat Autonoma de Barcelona, E-08193, Bellaterra (Barcelona), Spain*
[5]*Baylor University, Waco, Texas 76798, USA*
[6a]*Istituto Nazionale di Fisica Nucleare Bologna, I-40127 Bologna, Italy*
[6b]*University of Bologna, I-40127 Bologna, Italy*
[6]*Brandeis University, Waltham, Massachusetts 02254, USA*
[7]*University of California, Davis, Davis, California 95616, USA*
[8]*University of California, Los Angeles, Los Angeles, California 90024, USA*
[9]*University of California, San Diego, La Jolla, California 92093, USA*
[10]*University of California, Santa Barbara, Santa Barbara, California 93106, USA*
[11]*Instituto de Fisica de Cantabria, CSIC-University of Cantabria, 39005 Santander, Spain*
[12]*Carnegie Mellon University, Pittsburgh, Pennsylvania 15213, USA*
[13]*Enrico Fermi Institute, University of Chicago, Chicago, Illinois 60637, USA*
[14]*Comenius University, 842 48 Bratislava, Slovakia; Institute of Experimental Physics, 040 01 Kosice, Slovakia*
[15]*Joint Institute for Nuclear Research, RU-141980 Dubna, Russia*
[16]*Duke University, Durham, North Carolina 27708, USA*
[17]*Fermi National Accelerator Laboratory, Batavia, Illinois 60510, USA*
[18]*University of Florida, Gainesville, Florida 32611, USA*
[19]*Laboratori Nazionali di Frascati, Istituto Nazionale di Fisica Nucleare, I-00044 Frascati, Italy*
[20]*University of Geneva, CH-1211 Geneva 4, Switzerland*
[21]*Glasgow University, Glasgow G12 8QQ, United Kingdom*

[22]Harvard University, Cambridge, Massachusetts 02138
[23]Division of High Energy Physics, Department of Physics, University of Helsinki and Helsinki Institute of Physics,
FIN-00014, Helsinki, Finland
[24]University of Illinois, Urbana, Illinois 61801, USA
[25]The Johns Hopkins University, Baltimore, Maryland 21218, USA
[26]Institut für Experimentelle Kernphysik, Universität Karlsruhe, 76128 Karlsruhe, Germany
[27]Center for High Energy Physics: Kyungpook National University, Daegu 702-701, Korea;
Seoul National University, Seoul 151-742, Korea;
Sungkyunkwan University, Suwon 440-746, Korea;
Korea Institute of Science and Technology Information, Daejeon, 305-806, Korea;
Chonnam National University, Gwangju, 500-757, Korea
[28]Ernest Orlando Lawrence Berkeley National Laboratory, Berkeley, California 94720, USA
[29]University of Liverpool, Liverpool L69 7ZE, United Kingdom
[30]University College London, London WC1E 6BT, United Kingdom
[31]Centro de Investigaciones Energeticas Medioambientales y Tecnologicas, E-28040 Madrid, Spain
[32]Massachusetts Institute of Technology, Cambridge, Massachusetts 02139, USA
[33]Institute of Particle Physics: McGill University, Montreal, Canada H3A 2T8;
and University of Toronto, Toronto, Canada M5S 1A7
[34]University of Michigan, Ann Arbor, Michigan 48109, USA
[35]Michigan State University, East Lansing, Michigan 48824, USA
[36]Institution for Theoretical and Experimental Physics, ITEP, Moscow 117259, Russia
[37]University of New Mexico, Albuquerque, New Mexico 87131, USA
[38]Northwestern University, Evanston, Illinois 60208, USA
[39]The Ohio State University, Columbus, Ohio 43210, USA
[40]Okayama University, Okayama 700-8530, Japan
[41]Osaka City University, Osaka 588, Japan
[42]University of Oxford, Oxford OX1 3RH, United Kingdom
[44a]Istituto Nazionale di Fisica Nucleare, Sezione di Padova-Trento, I-35131 Padova, Italy
[44b]University of Padova, I-35131 Padova, Italy
[43]LPNHE, Universite Pierre et Marie Curie/IN₂P₃-CNRS, UMR7585, Paris, F-75252, France
[44]University of Pennsylvania, Philadelphia, Pennsylvania 19104, USA
[47a]Istituto Nazionale di Fisica Nucleare Pisa, I-56127 Pisa, Italy
[47b]University of Pisa, I-56127 Pisa, Italy
[47c]University of Siena, I-56127 Pisa, Italy
[47d]Scuola Normale Superiore, I-56127 Pisa, Italy
[48]University of Pittsburgh, Pittsburgh, Pennsylvania 15260, USA
[49]Purdue University, West Lafayette, Indiana 47907, USA
[50]University of Rochester, Rochester, New York 14627, USA
[51]The Rockefeller University, New York, New York 10021, USA
[52a]Istituto Nazionale di Fisica Nucleare, Sezione di Roma 1, I-00185 Roma, Italy
[52b]Sapienza Università di Roma, I-00185 Roma, Italy
[53]Rutgers University, Piscataway, New Jersey 08855, USA
[54]Texas A&M University, College Station, Texas 77843, USA
[55a]Istituto Nazionale di Fisica Nucleare Trieste/Udine, Italy
[55b]University of Trieste/Udine, Italy
[56]University of Tsukuba, Tsukuba, Ibaraki 305, Japan
[57]Tufts University, Medford, Massachusetts 02155, USA
[58]Waseda University, Tokyo 169, Japan
[59]Wayne State University, Detroit, Michigan 48201, USA
[60]University of Wisconsin, Madison, Wisconsin 53706, USA
[61]Yale University, New Haven, Connecticut 06520, USA
(Received 1 August 2008; published 14 April 2009)

We report a measurement of the top-quark mass M_t in the dilepton decay channel $t\bar{t} \rightarrow bl'^+ \nu'_l \bar{b} l^- \bar{\nu}_l$. Events are selected with a neural network which has been directly optimized for statistical precision in top-quark mass using neuroevolution, a technique modeled on biological evolution. The top-quark mass is extracted from per-event probability densities that are formed by the convolution of leading order matrix elements and detector resolution functions. The joint probability is the product of the probability densities from 344 candidate events in 2.0 fb^{-1} of $p\bar{p}$ collisions collected with the CDF II detector, yielding a measurement of $M_t = 171.2 \pm 2.7\text{(stat)} \pm 2.9\text{(syst)}$ GeV/c^2.

Over ten years after the discovery of the top quark, its mass, M_t, remains a quantity of great interest. M_t-dependent terms contribute to radiative corrections to precision electroweak observables, thus providing information on the unobserved Higgs boson [1] and other particles in possible extensions to the standard model [2] (SM). Top quarks are produced only at the Fermilab Tevatron, primarily in pairs and decay $\approx 100\%$ to a W boson and a b quark, $t\bar{t} \rightarrow W^+ b W^- \bar{b}$, in the SM. The dilepton channel, where both W bosons decay to charged leptons (electrons and muons, including leptonic decays of τ leptons) and neutrinos, has the smallest branching fraction, but also has the least number of hadronic jets in the final state and hence a smaller sensitivity to their energy calibration. Significant differences in the measurements of M_t in different decay channels could indicate contributions from sources beyond the SM [3].

Reconstruction of M_t in the dilepton channel presents unique challenges, as the two neutrinos in the final state result in a kinematically underconstrained system. We utilize a likelihood-based estimator that convolutes leading order SM matrix elements and detector resolution functions and integrates over unmeasured quantities. Prior applications of this method to dilepton events have yielded the most precise measurements of M_t in this channel [4–6]. These prior measurements utilize event selection criteria that were designed to maximize signal purity for a measurement of the $t\bar{t}$ production cross section [7]. The selection optimization for precision in M_t is hampered by the difficulty of searching the space of arbitrary multivariate selections. Well established multivariate algorithms such as neural networks are typically limited to minimization of a specific metric, such as misclassification error. They are not designed to optimize an event ensemble property, such as the uncertainty on the top-quark mass. In contrast, the technique of neuroevolution [8] combines the parametrization of an abitrary multivariate selection described by a neural network with an evolutionary minimization approach to search for the network weights and topology which optimizes an arbitrary metric. In this Letter, we present a measurement using an improved matrix element analysis technique and an event selection optimized with neuroevolution to minimize the expected statistical uncertainty in the top-quark mass measurement. We utilize 2.0 fb^{-1} of data collected between March 2002 and May 2007 with the CDF II detector at the Fermilab Tevatron.

CDF II [9–11] contains a charged particle tracking system consisting of a silicon microstrip tracker and a drift chamber immersed in a 1.4 T magnetic field. Surrounding electromagnetic and hadronic calorimeters measure particle energies. Outside the calorimeters, drift chambers and scintillators detect muons.

We use lepton triggers that require an electron or muon with $p_T > 18 \text{ GeV}/c$. We define a preselection which satisfies the basic signature of top dilepton decay: two oppositely charged leptons with $p_T > 20 \text{ GeV}/c$, two or more jets with $E_T > 15 \text{ GeV}$ [12] within the region $|\eta| < 2.5$, $\not{E}_T > 20 \text{ GeV}$ [13], and dilepton invariant mass $M_{ll} > 10 \text{ GeV}/c^2$. Suppression of the $Z \rightarrow ll$ background is performed by the subsequent neural-network selection.

Neuroevolution, an approach modeled on biological evolution, is used to search directly for the optimal neural network. Beginning with a population of 150 networks with random weights, the statistical precision of M_t is evaluated for each network by performing experiments using the simulated signal and background events which survive a threshold requirement on the network output. The events are simulated using the PYTHIA [14] and ALPGEN [15] generators and a full detector simulation [16]. Poorly performing networks are culled, and the 30 strongest performers are bred together and mutated in successive generations until performance reaches a plateau in a statistically independent pool of events, which occurs after 15 generations. The statistical uncertainty obtained from the best performer in each generation is shown in Fig. 1(a). In the context of an arbitrary but *a priori* fixed choice of network threshold, the networks evolve to optimize the selection regardless of the threshold's value. Because we have optimized directly on the final statistical precision rather than some intermediate or approximate figure of merit, the best-performing network is the one which gives the most precise measurement. This approach has been shown to significantly outperform traditional methods in event selection [17]. In particular, we use neuroevolution of augmenting topologies [18], a neuroevolutionary method capable of evolving a network's topology and weights.

Some of the events passing this selection have secondary vertex tags [19], which enhance the b-quark fraction and thus signal purity. We exploit this enhancement by separately fitting events with and without secondary vertex tags, and combining the fits. The predicted number of signal and background events is shown in Table I. Using the optimized selection improves the *a priori* statistical uncertainty on M_t over the selection used in previous analyses [6] by 20%. This neural-network selection yields 344 candidate events (Fig. 2). Strikingly, the sample selected by the neural network is expected to be dominated by background events; the resulting measurement is expected to be more precise than previous measurements due to the increase in $t\bar{t}$ acceptance and the suppression of background effects as described below. The distribution of expected statistical uncertainty versus signal purity for all evaluated networks can be seen in Fig. 1(b).
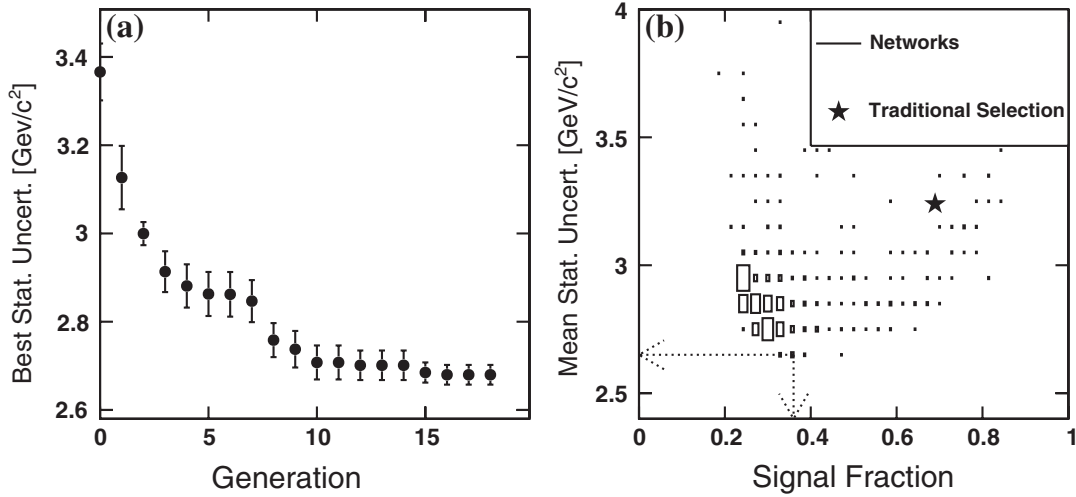
FIG. 1. (a) Expected statistical uncertainty for the best network in each successive generation of network evaluation. The points show the average performance for each generation; the error bars show the variation due to the randomly generated networks in generation 0. (b) Expected statistical uncertainty on M_t versus signal fraction after neural-network selection, for all evaluated networks. The selection [7] used in previous measurements is shown ($\star$) for comparison. The arrows show the expected statistical uncertainty and signal fraction corresponding to the network used in the analysis.

We express the probability density for the observed lepton and jet measurements, $\mathbf{x}_i$, as a function of the top-quark mass M_t as $P_s(\mathbf{x}_i|M_t)$. We calculate $P_s(\mathbf{x}_i|M_t)$ using the theoretical description of the $t\bar{t}$ production and decay process with respect to $\mathbf{x}_i$, $P_s(\mathbf{x}_i|M_t) = [1/\sigma(M_t)] \times [d\sigma(M_t)/d\mathbf{x}_i]$, where $\frac{d\sigma}{d\mathbf{x}_i}$ is the differential cross section [20–22] and σ is the total cross section. The term $1/\sigma(M_t)$ ensures that the probability density satisfies the normalization condition, $\int d\mathbf{x}_i P_s(\mathbf{x}_i|M_t) = 1$.

We evaluate $P_s(\mathbf{x}_i|M_t)$ [6] by integrating over quantities that are not directly measured, such as neutrino momenta and quark energies. The effect of simplifying assumptions is estimated using simulated experiments. We integrate over quark energies using a parametrized detector transfer function [5] $W(p, j)$, defined as the probability of measuring jet energy j given quark energy p.

We account for backgrounds using their probability densities $P_{\mathrm{bg}_k}(\mathbf{x}_i)$ and form the full per-event probability

$$P^n(\mathbf{x}_i|M_t) = P_s(\mathbf{x}_i|M_t)p_s^n + \sum_k P_{\mathrm{bg}_k}(\mathbf{x}_i)p_{\mathrm{bg}_k}^n. \quad (1)$$

The functions $P_{\mathrm{bg}_k}(\mathbf{x}_i)$ are calculated using the differential cross section for each background. The proportions p_s^n and $p_{\mathrm{bg}_k}^n$ depend on whether the event has n secondary vertex tags, and are obtained from Table I. We evaluate background probability densities for $Z/\gamma^*(\to ee, \mu\mu)$ + jets, $W + \geq 3$ jets where a jet is misidentified as a lepton, and WW + jets. Probability densities for smaller backgrounds
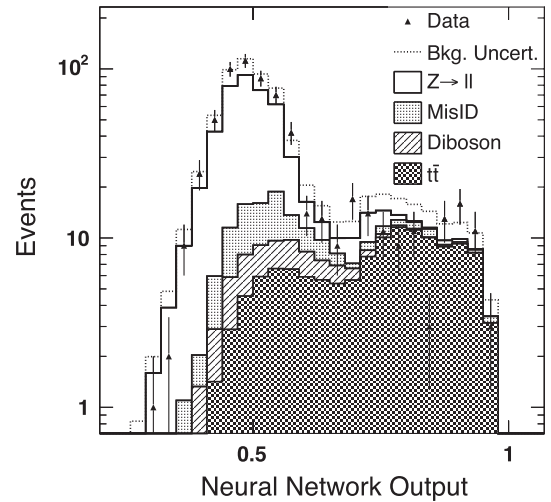

FIG. 2. The output of the final network evaluated on the collected data (black triangles), with expected signal and background contributions (stacked solid histograms). The data show events passing the preselection. The evolution of the optimum selection network is performed with an *a priori* threshold set at 0.5 for candidate selection. Of the 642 preselected events shown, 344 events pass this threshold and constitute the final candidate sample for mass fitting.
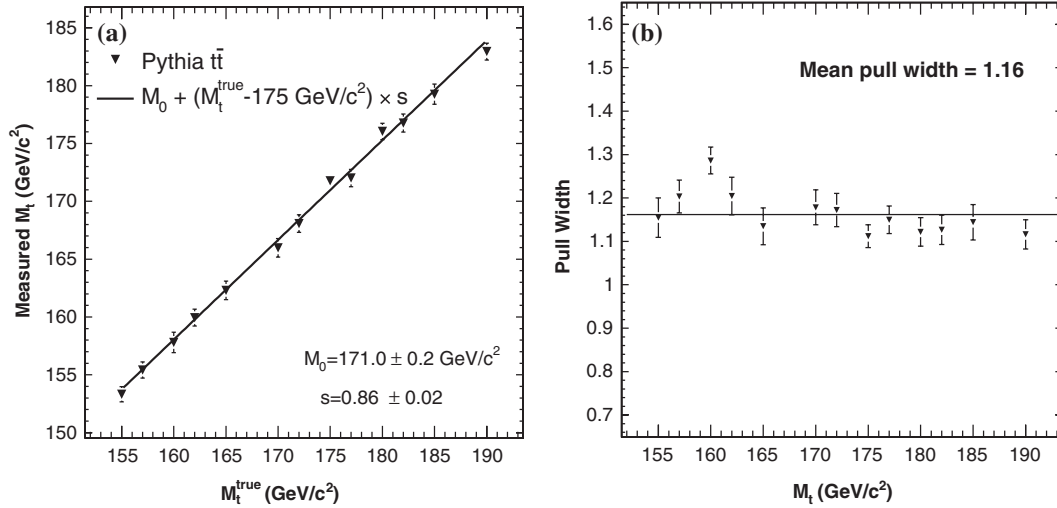
TABLE I. Expected sample composition after neural-network selection for events with and without secondary vertex tags.

Source	N(0 tag)	$N(\geq 1$ tag)
$Z \to ll$	116.5 ± 18.6	4.1 ± 1.8
$Z \to ll + c\bar{c}/b\bar{b}$	9.3 ± 1.4	10.1 ± 4.0
$WW, WZ, ZZ, W\gamma$	17.3 ± 5.9	0.7 ± 0.7
Misidentified leptons	29.0 ± 8.7	4.5 ± 1.1
$t\bar{t}$ ($\sigma = 6.7$ pb, $M_t = 175$ GeV/c^2)	43.8 ± 4.4	78.0 ± 6.2
Total	215.8 ± 21.9	97.5 ± 7.2
Observed (2.0 fb^{-1})	246	98

FIG. 3. (a) Mean measured M_t in simulated experiments versus top-quark masses. The solid line is a linear fit to the points. (b) Pull widths from simulated experiments versus top-quark masses. The solid line is the average over all points.

(WZ, ZZ, $W\gamma$, and $Z \to \tau\tau$) provide negligible gain in sensitivity and are not modeled.

The posterior joint probability for the sample is the product of the per-event probability densities,

$$P(\mathbf{x}|M_t) = \left[\prod_{i_0} P^0(\mathbf{x}_{i_0}|M_t) \right]\left[\prod_{i_1} P^{\geq 1}(\mathbf{x}_{i_1}|M_t) \right] \quad (2)$$

over all untagged (i_0) and tagged (i_1) events. The measured mass M_t is taken as the mean $\langle M_t \rangle$ computed using the posterior probability, and the measured statistical uncertainty ΔM_t is taken as the standard deviation.

The response of our method for simulated experiments [Fig. 3(a)] is consistent with a linear dependence on the true top mass. Its slope is less than unity due to the presence of unmodeled background. We derive corrections, $M_t \to 175.0$ GeV/c^2 + (M_t − 171.0 GeV/c^2)/0.86 and $\Delta M_t \to \Delta M_t/0.86$, from this response and apply them to the measured quantities in data.

From the pull distribution of our simulated experiments, we find that ΔM_t is underestimated [Fig. 3(b)]. This is due to simplifying assumptions made in the probability calculations for computational tractability [5]. These assumptions are violated in small, well-understood ways in realistic events. We scale ΔM_t by an additional factor, $S = 1.16$, derived from our simulated experiments. Applying this method to the 344 candidate events, we measure $M_t = 171.2 \pm 2.7$(stat) GeV/c^2. The posterior probability is Gaussian within the statistical accuracy of the Monte Carlo integration.

There are several sources of systematic uncertainty in our measurement, which are summarized in Table II. The single largest source of systematic error comes from the uncertainty in the jet energy scale, which we estimate to be 2.5 GeV/c^2 by varying the scale within its uncertainty [23]. An uncertainty specific to jets resulting from b par-

tons contributes 0.4 GeV/c^2, while in-time pileup contributes 0.2 GeV/c^2. Uncertainty due to the Monte Carlo generator used for $t\bar{t}$ events is estimated as the difference in M_t extracted from PYTHIA events and HERWIG [24] events and amounts to 0.9 GeV/c^2. Uncertainties due to parton distribution functions are estimated using different parton distribution function sets (CTEQ5L [25] vs MRST72 [26]), using different values of Λ_{QCD}, and varying the eigenvectors of the CTEQ6M [25] set; the quadrature sum of the last two (dominant) uncertainties is 0.6 GeV/c^2. The limited number of background events available for simulated experiments results in an uncertainty on the shape of the background distributions, which yields an uncertainty on M_t of 0.5 GeV/c^2. Uncertainty due to imperfect modeling of initial (ISR) and final (FSR) QCD radiation is estimated by varying the amounts of ISR and FSR in simulated events [27] and is estimated to be 0.5 GeV/c^2. The uncertainty in the mass due to uncertainties in the

TABLE II. Summary of systematic uncertainties on the measured top-quark mass.

Source	Size (GeV/c^2)
Generic jet energy scale	2.5
b-jet energy scale	0.4
In-time pileup	0.2
Generator	0.9
Parton distribution functions	0.6
Background statistics	0.5
Radiation	0.5
Response correction	0.4
Sample composition uncertainty	0.3
Background modeling	0.2
Lepton energy scale	0.1
Total	2.9

response correction is evaluated by varying the response within the uncertainties shown in Fig. 3(a) and is 0.4 GeV/c^2. The contribution from uncertainties in background composition is estimated by varying the background normalizations from Table I within their uncertainties and amounts to 0.3 GeV/c^2. We estimate the uncertainty coming from modeling of the missing tranverse energy in Z/γ^* events and the uncertainty in the data-derived model of misidentified leptons to be 0.2 GeV/c^2. The uncertainty in the lepton energy scale contributes an uncertainty of 0.1 GeV/c^2 to our measurement. Adding in quadrature yields a total systematic uncertainty of 2.9 GeV/c^2.

In summary, we have presented a new measurement of the top-quark mass in the dilepton channel. We have applied the technique of neuroevolution, for the first time in particle physics, to devise an event selection criterion which optimizes statistical precision. We measure $M_t = 171.2 \pm 2.7(\text{stat}) \pm 2.9(\text{syst})$ GeV/c^2. This is the single most precise measurement of M_t in this channel to date, is in good agreement with measurements in other channels [28,29], and represents a $\sim 30\%$ improvement in statistical precision over the previously published measurements in this channel [6,30,31].

[a]Deceased.
[b]With visitors from Universiteit Antwerpen, B-2610 Antwerp, Belgium.
[c]With visitors from Chinese Academy of Sciences, Beijing 100864, China.
[d]With visitors from University of Bristol, Bristol BS8 1TL, United Kingdom.
[e]With visitors from University of California Irvine, Irvine, California 92697, USA.
[f]With visitors from University of California Santa Cruz, Santa Cruz, California 95064, USA.
[g]With visitors from Cornell University, Ithaca, New York 14853, USA.
[h]With visitors from University of Cyprus, Nicosia CY-1678, Cyprus.
[i]With visitors from University College Dublin, Dublin 4, Ireland.
[j]With visitors from University of Edinburgh, Edinburgh EH9 3JZ, United Kingdom.
[k]With visitors from Universidad Iberoamericana, Mexico Distrito Federal, Mexico.
[l]With visitors from University of Manchester, Manchester M13 9PL, England.
[m]With visitors from Nagasaki Institute of Applied Science, Nagasaki, Japan.
[n]With visitors from University de Oviedo, E-33007 Oviedo, Spain.
[o]With visitors from Queen Mary, University of London, London, E1 4NS, England.
[p]With visitors from Texas Tech University, Lubbock, Texas 79409, USA.
[q]With visitors from IFIC (CSIC-Universitat de Valencia), 46071 Valencia, Spain.
[r]With visitors from Royal Society of Edinburgh/Scottish Executive Support Research Fellow.
[s]With visitors from Istituto Nazionale di Fisica Nucleare, Sezione di Cagliari, 09042 Monserrato (Cagliari), Italy.
[t]With visitors from Informatics Institute, University of Amsterdam, Amsterdam, The Netherlands.

[1] LEP Collaboration, LEP Electroweak Working group, SLD Electroweak and Heavy Flavor Groups (LEP), CERN Report No. CERN-PH-EP/2007-039, 2007.
[2] S. Heinemeyer *et al.*, J. High Energy Phys. 09 (2003) 075.
[3] G. L. Kane and S. Mrenna, Phys. Rev. Lett. **77**, 3502 (1996).
[4] A. Abulencia *et al.* (CDF Collaboration), Phys. Rev. Lett. **96**, 152002 (2006).
[5] A. Abulencia *et al.* (CDF Collaboration), Phys. Rev. D **74**, 032009 (2006).
[6] A. Abulencia *et al.* (CDF Collaboration), Phys. Rev. D **75**, 031105 (2007).
[7] D. Acosta *et al.* (CDF Collaboration), Phys. Rev. Lett. **93**, 142001 (2004).
[8] X. Yao, Proc. IEEE **87**, 1423 (1999).
[9] D. Acosta *et al.* (CDF Collaboration), Phys. Rev. D **71**, 032001 (2005).
[10] A. Abulencia *et al.* (CDF Collaboration), J. Phys. G **34**, 2457 (2007).
[11] CDF uses a cylindrical coordinate system with the z axis along the proton beam axis. Pseudorapidity is $\eta \equiv -\ln(\tan\theta/2)$, θ (ϕ) is the polar (azimuthal) angle relative to the z axis, while $p_T = |p|\sin\theta$, $E_T = E\sin\theta$.
[12] F. Abe *et al.* (CDF Collaboration), Phys. Rev. D **45**, 1448 (1992).
[13] Missing transverse energy $\not{E}_T \equiv |-\sum_i E_T^i \vec{n}_i|$, where E_T^i is the transverse energy in calorimeter tower i, and $\vec{n}_i$ is the unit transverse vector from the beam line to tower i.

[14] T. Sjostrand *et al.*, Comput. Phys. Commun. **135**, 238 (2001).

[15] M. L. Mangano *et al.*, J. High Energy Phys. 07 (2003) 001.

[16] T. Affolder *et al.*, Nucl. Instrum. Methods Phys. Res., Sect. A **447**, 1 (2000).

[17] S. Whiteson and D. Whiteson, in *Proceedings of the Twenty-Second AAAI Conference on Artificial Intelligence, 2007, Vancouver, British Columbia, Canada* (AAAI Press, Menlo Park, CA, 2007), ISBN .

[18] K. O. Stanley and R. Miikkulainen, Evolutionary Computation **10**, 99 (2002).

[19] D. Acosta *et al.* (CDF Collaboration), Phys. Rev. D **71**, 052003 (2005).

[20] G. Mahlon and S. Parke, Phys. Lett. B **411**, 173 (1997).

[21] G. Mahlon and S. Parke, Phys. Rev. D **55**, 7249 (1997).

[22] While $\approx 15\%$ of $t\bar{t}$ are produced by gluon-gluon fusion ($gg \rightarrow t\bar{t}$), it has negligible effect on our measurement.

[23] A. Bhatti *et al.*, Nucl. Instrum. Methods Phys. Res., Sect. A **566**, 375 (2006).

[24] G. Corcella *et al.*, J. High Energy Phys. 01 (2001) 010.

[25] J. Pumplin *et al.*, J. High Energy Phys. 07 (2002) 012.

[26] A. D. Martin *et al.*, Phys. Lett. B **356**, 89 (1995).

[27] A. Abulencia *et al.* (CDF Collaboration), Phys. Rev. D **73**, 032003 (2006).

[28] T. Aaltonen *et al.* (CDF Collaboration), Phys. Rev. Lett. **99**, 182002 (2007).

[29] T. Aaltonen *et al.* (CDF Collaboration), Phys. Rev. D **76**, 072009 (2007).

[30] T. Aaltonen *et al.* (CDF Collaboration), Phys. Rev. Lett. **100**, 062005 (2008).

[31] V. Abazov *et al.* (D0 Collaboration), Phys. Lett. B **655**, 7 (2007).